AJNR

Diagnostic Utility of 3D Gradient-Echo MR Imaging Sequences through the Filum Compared with Spin-Echo T1 in Children with Concern for Tethered Cord

F. Rafiee, W.A. Mehan, S. Rincon, S. Rohatgi, O. Rapalino and K. Buch

AJNR Am J Neuroradiol published online 16 February 2023
http://www.ajnr.org/content/early/2023/02/16/ajnr.A7791

Published February 16, 2023 as 10.3174/ajnr.A7791

Diagnostic Utility of 3D Gradient-Echo MR Imaging Sequences through the Filum Compared with Spin-Echo T1 in Children with Concern for Tethered Cord

F. Rafiee, W.A. Mehan, S. Rincon, S. Rohatgi, O. Rapalino, and K. Buch

ABSTRACT

BACKGROUND AND PURPOSE: Fatty intrathecal lesions are a cause of tethered cord, and detection of these on spinal MR imaging is paramount. Conventional T1 FSE sequences are the mainstay of detecting fatty elements; however, 3D gradient-echo MR images, volumetric interpolated breath-hold examination/liver acquisition with volume acceleration (VIBE/LAVA), are popular, given the increased motion resistance. We sought to evaluate the diagnostic accuracy of VIBE/LAVA compared with T1 FSE for detection of fatty intrathecal lesions.

MATERIALS AND METHODS: In this retrospective, institutional review board–approved study, 479 consecutive pediatric spine MRIs obtained to evaluate cord tethering between January 2016 and April 2022 were reviewed. Inclusion criteria were patients who were 20 years of age or younger who underwent spine MRIs containing both axial T1 FSE and VIBE/LAVA sequences of the lumbar spine. The presence or absence of fatty intrathecal lesions was recorded for each sequence. If fatty intrathecal lesions were present, anterior-posterior and transverse dimensions were recorded. VIBE/LAVA and T1 FSE sequences were evaluated on 2 separate occasions (VIBE/LAVAs first followed by T1 FSE several weeks later) to minimize bias. Basic descriptive statistics compared fatty intrathecal lesion sizes on T1 FSEs and VIBE/LAVAs. Receiver operating characteristic curves were used to determine minimal fatty intrathecal lesion size detectable by VIBE/LAVA.

RESULTS: Sixty-six patients were included, with 22 having fatty intrathecal lesions (mean age, 7.2 years). T1 FSE sequences revealed fatty intrathecal lesions in 21/22 cases (95%); however, fatty intrathecal lesions on VIBE/LAVA were detected in 12/22 patients (55%). Mean anterior-posterior and transverse dimensions of fatty intrathecal lesions measured larger on T1 FSE compared with VIBE/LAVA sequences (5.4 × 5.0 mm versus 1.5 × 1.6 mm, respectively; *P* values = .039 anterior-posterior; .027 transverse).

CONCLUSIONS: While T1 3D gradient-echo MR images may have decreased the acquisition time and are more motion-resistant than conventional T1 FSE sequences, they are less sensitive and may miss small fatty intrathecal lesions.

ABBREVIATIONS: AP = anterior-posterior; FIL = fatty intrathecal lesion; LAVA = liver acquisition with volume acceleration; RL = transverse; ROC = receiver operating characteristic; TCS = tethered cord syndrome; VIBE = volumetric interpolated breath-hold examination

Tethered cord syndrome (TCS) is a progressive neurologic condition that develops because of excessive tension on the spinal cord often related to the presence of a filar lesion. If untreated, patients may incur ischemic injury and diminished nerve conduction followed by motor and sensory deficits.[1,2] Early detection with MR imaging and early surgical intervention are of paramount importance for preserving the quality of life in affected children.[1,3-5] Filar lesions include deposition of abnormal fatty tissue within the filum terminale and intradural/intrathecal lipomas, which can lead to impaired cord ascent and excessive stress on the conus.[6]

MR imaging is the mainstay for detection of abnormal conus position, characterization of findings suggestive of TCS, and presurgical planning.[7-9] Fatty intrathecal lesions (FILs), including both fatty fila and intraspinal lipomas, have traditionally been detected on T1 FSE sequences.[10] Gewirtz et al[11] published a series of fast MR imaging protocols for pediatric spine imaging using T2-weighted HASTE, T1-weighted TSE, and T2-weighted STIR sequences. The authors concluded that this set of MR images can identify spinal dysraphisms and other intraspinal anomalies. Sankhe et al[12] evaluated the utility of the CISS sequence for the detection of TCS, concluding that CISS is superior for detecting tethering elements, given the excellent spatial resolution and high

Received October 31, 2022; accepted after revision January 9, 2023.

From the Department of Radiology, Massachusetts General Hospital, Harvard Medical School, Boston, Massachusetts.

Please address correspondence to Karen Buch, MD, Harvard Medical School, Department of Radiology, Massachusetts General Hospital, 55 Fruit St, Boston, MA 02114; e-mail: kbuch@partners.org

http://dx.doi.org/10.3174/ajnr.A7791

contrast between CSF and soft-tissue structures. However, the CISS acquisition time is much longer than that of the T2 sequences and is less sensitive for the detection of fat elements. Despite these prior publications, the best fast sequence for detection of FILs is yet to be determined.[11,13] In most radiologists' practices, T1-weighted images are the mainstay of the MR images in detecting fat elements in spinal anomalies.[14]

Recently, there has been an emphasis on fast-acquisition sequences, which are more resistant to motion artifacts, a feature that is particularly desirable for pediatric imaging. As a 3D T1-weighted gradient-echo sequence, volumetric interpolated breath-hold examination (VIBE) reduces the motion artifacts by its unique *k*-space sampling scheme.[15,16] This sequence generates T1-weighted images but uses a spoiled gradient-echo sequence with ultrashort TRs and has shown lower signal-to-noise ratios compared with spin-echo imaging in prior studies.[16-18] VIBE/liver acquisition with volume acquisition (LAVA) has been shown to be superior to T1-weighted FSE for the detection of pediatric spinal leptomeningeal lesions, owing to its shorter acquisition time and fewer motion artifacts related to respiration, cardiac motion, vessel pulsation, and CSF flow.[19] Because there is a lack of consensus on the best way to evaluate TCS, we sought to compare the diagnostic utility of the VIBE/LAVA sequence for the detection of FILs in the pediatric age group with an FSE T1 pulse sequence. We hypothesized that the VIBE/LAVA will not be as sensitive for the detection of FILs compared with conventional T1 FSE sequences and may miss small FILs.

MATERIALS AND METHODS

This was an institutional review board–approved, retrospective study performed at a single institution. Using a keyword database search, we identified sequential pediatric MR imaging spine studies performed to evaluate cord tethering at our institution during a 6-year period spanning January 2016 to April 2022. Inclusion criteria were the following: 1) patients younger than 20 years of age undergoing spine MR imaging for clinically suspected TCS, and 2) MR imaging acquisition including both conventional T1 FSE and VIBE/LAVA sequences through the lumbar spine. Patients were excluded if the imaging was degraded by motion artifacts that precluded a diagnostic assessment.

MR imaging examinations of the spine were performed on either a 1.5T (Signa HDxt; GE Healthcare) or 3T platform (Magnetom Prisma Fit; Siemens). Acquired sequences used in this study included sagittal and axial T1 FSE sequences, T2WI, and axial ultrafast spoiled gradient-echo sequences known as VIBE on Siemens scanner and LAVA on GE scanner. In our study, we use the term VIBE/LAVA to address the T1-weighted 3D gradient-echo MR images from both vendors.

For the 1.5T GE platform, the MR imaging parameters for axial T1 FSE were as follows: TE = 11.696 ms, TR = 623 ms, section thickness = 3, matrix = 384 × 256, FOV = 100, scan time = 2.1 minutes, number of excitations = 1, flip angle = 90°, echo-train length = 3. The same parameters for axial LAVA were TE = 2.516 ms, TR = 5.072 ms, section thickness = 3 mm, matrix = 320 × 224, FOV = 100 mm, scan time = 2.25 minutes, number of excitations = 0.74, echo-train length = 1, flip angle = 15°.

For the 3T Siemens platform, the MR imaging parameters for axial T1 FSE were as follows: TE = 10 ms, TR = 545 ms, section thickness = 3, matrix = 256 × 230, FOV = 100, scan time = 1.7 minutes, number of excitations = 1, flip angle = 120°, turbo factor = 3. The same parameters for axial VIBE were TE = 1.61 ms, TR = 4.16 ms, section thickness = 1, matrix = 256 × 256, FOV = 100, scan time = 1.7 minutes, number of excitations = 2, turbo factor = 1, flip angle = 15°.

All MR imaging examinations were evaluated using Visage 7, Version 7.1.9c (Visage Imaging). The presence of a FIL was defined as a T1-hyperintense structure extending along the course of the filum terminale. FILs included both fatty fila as well as intradural lipomas. Each MR imaging was independently evaluated by 2 radiologists who were blinded to the clinical and surgical outcomes: 1) a pediatric neuroradiologist with 5 years of experience, and 2) a radiologist (K.B.) with >5 years of practice. For each patient, we recorded the following data: 1) basic demographic information including age, sex, presenting signs and symptoms, 2) the presence/absence of a FIL as determined on conventional T1 FSE, and 3) the presence/absence of a FIL as seen on VIBE/LAVA sequences (Figs 1 and 2).

To avoid a potential source of bias, we reviewed the T1 FSE and VIBE/LAVA sequences at 2 separate points in time. During both rounds of review, the readers were blinded to the radiology report, clinical history, and assessment for FILs on other sequences. The VIBE/LAVA sequence was assessed during the first round, and at least 2 weeks later, the conventional T1 FSE sequences were reviewed. For both the conventional T1 FSE sequence and the VIBE/LAVA sequence, if a FIL was present, the maximal axial anterior-posterior (AP) and transverse (RL) measurements were recorded as measured in the axial plane. Craniocaudal dimensions were measured as the number of vertebral body segments spanned.

Statistical Analysis

All statistical analyses were performed using SPSS, Version 28.0.0 (IBM). Independent *t* tests were used to compare the AP and RL diameters of FILs seen on T1 FSE sequences, which were also detected on VIBE/LAVA sequences, compared with FILs seen only on T1 FSE and not on VIBE/LAVA sequences.

A paired *t* test was used to compare the AP and RL measurements of FILs detected on VIBE/LAVA sequences with the corresponding measurements on T1 FSE sequences. Independent and paired *t* tests were similarly used for calculating the correlation between the craniocaudal extension of the FIL in both sequences.

Finally, to find a cutoff value for FIL size in which VIBE/LAVA can detect the lesion with an acceptable sensitivity and specificity, we illustrated the performance of a classification model at all classification thresholds by drawing a receiver operating characteristic (ROC) curve.

Interrater agreement between the radiologists was determined in both the FIL dimension and craniocaudal extension measurements, by calculating the intraclass correlation coefficient.

RESULTS

A total of 479 patient examinations performed between January 2016 and April 2022 were reviewed. A total of 66 patients (0–20 years of age) met the inclusion criteria. Of these 66 patients, 22 patients

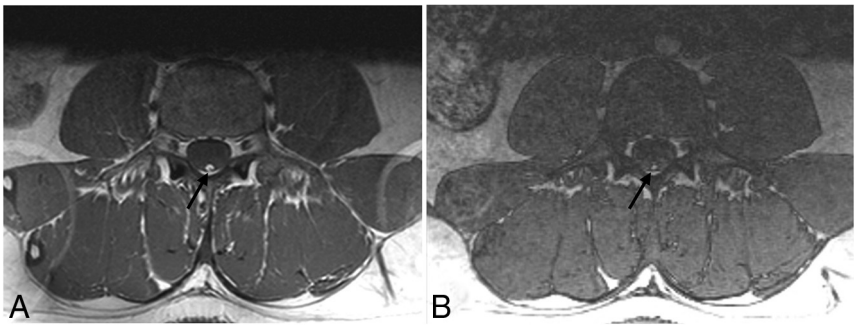

FIG 1. Different acquisitions of T1-weighted MR imaging on the axial planes of the lumbar region at the level of the L4–L5 intervertebral disc in an 18-year-old patient. *A*, T1 FSE sequence shows the dark-signal thecal sac containing the barely visible hypo- to iso-signal intensity cauda equina nerve roots and a round midline intradural lesion (*black arrow*) with bright signal intensity located posteriorly in the spinal canal at the expected anatomic site of the filum terminale, consistent with a FIL. Phase wrap-around artifacts are noted on both sides of the image. *B*, A radiofrequency spoiled 3D gradient-echo sequence known as VIBE of the same patient study at the same level shows a similar bright-signal intradural structure (*black arrow*), the FIL. Note the smaller AP and RL dimensions of the FIL compared with the T1 FSE sequence (*A*). The cauda equina nerve roots are well-demarcated as opposed to the T1 FSE sequence (*A*). VIBE/LAVA can underrate the AP and RL diameters of the FILs.

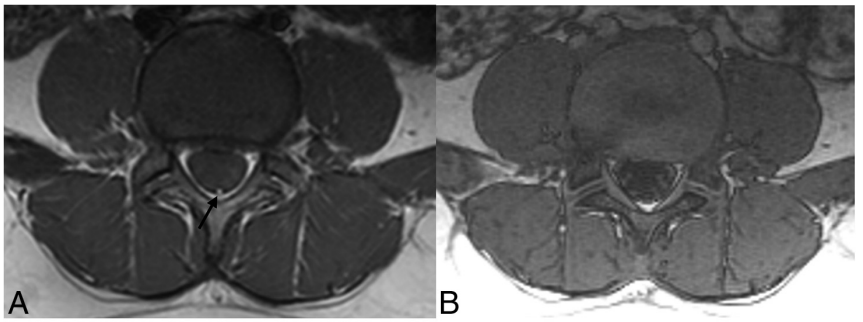

FIG 2. Different acquisitions of T1-weighted MR imaging on the axial plane through the lumbar region at the L4–L5 intervertebral disc in a 10-year-old boy. *A*, A T1 FSE sequence shows a tiny, round, midline intradural lesion (*black arrow*) with bright signal intensity located posteriorly in the spinal canal at the expected anatomic site of the filum terminale, consistent with a FIL. *B*, VIBE of the same patient at the same level shows iso-signal intensity nerve roots of the cauda equina traversing the spinal canal. Although the window level and width are adjusted for better detection of bright lesions, the VIBE sequence failed to reveal the FIL. Note the smaller AP and RL dimensions of the FIL compared with the case in Fig 3. The VIBE sequence is less sensitive in the detection of small FILs and can miss such lesions.

Table 1: Presenting sign and/or symptoms

Indication for MR Imaging	Total	FIL +ve	FIL −ve
Sacral abnormality	16 (24.2%)	9 (40.9%)	7 (16%)
Urinary dysfunction	10 (15.1%)	5 (22.7%)	5 (11.3%)
Bowel dysfunction	8 (12.1%)	2 (9%)	6 (13.6)
Scoliosis	7 (10.6%)	2 (9%)	5 (11.3%)
Lower-extremity weakness	6 (9%)	1 (4.5%)	5 (11.3%)
Back pain	6 (9%)	1 (4.5%)	5 (11.3%)
Other[a]	13 (19.5%)	2 (9%)	11 (25%)
Total	66	22	44

Note:—FIL +ve indicates positive detection of a FIL; FIL −ve, negative detection of a FIL.

[a] Other indications for MR imaging include abnormal gait, Chiari I malformation, abnormal findings on spine sonography, and vertebral defects, anal atresia, cardiac defects, tracheo-esophageal fistula, renal anomalies, and limb abnormalities (VACTERL).

had imaging findings consistent with a FIL on at least 1 sequence (either the conventional T1 FSE and/or the VIBE/LAVA).

The mean age in our cohort was 7.2 years (range, 2 days to 18.5 [SD, 5.7] years). For patients with FILs, the mean age was 6.8 years (range, 2 days- to 18.5 [SD, 6.3] years). The cohort included 33 males and 33 females.

The most common presenting sign in the affected group was an asymptomatic sacral region abnormality detected by physical examination (40.9%). These sacral region abnormalities included a visible sacral dimple, a palpable sacral mass, or a gluteal cleft asymmetry. Urinary dysfunction (22.7%), bowel dysfunction (9%), back pain (4.5%), lower extremity weakness (4.5%), and scoliosis (9%) were the most common symptoms (Table 1). Two patients (9%) underwent spinal imaging due to other medical conditions and had atypical symptoms for TCS.

T1 FSE sequences revealed FILs in 21/22 patients (95.4%), whereas VIBE/LAVA sequences detected FILs in 12/22 patients (54.5%) (Table 2 and Figs 1 and 2). At surgery, 21/22 (95.5%) of these cases had gross fatty elements found to be consistent with FILs. One of the patients with no imaging sign of FILs on either sequence (T1 FSE and VIBE/LAVA) underwent an operation for a tethered cord release, and fibrofatty tissue was evident at histopathology.

For cases with a suspected FIL on both T1 FSE and the VIBE/LAVA sequences, the mean AP and RL diameters were 5.40 and 5.02 mm, respectively.

For cases with a suspected FIL on T1 FSE sequences on which no intrinsically T1-bright focus was identified on the VIBE/LAVA sequence, the mean AP and RL diameters were 1.47 and 1.64 mm, respectively (Table 2). These dimensions demonstrate the lower size limit for detectable FILs on the VIBE/LAVA sequence (independent *t* test, *P* value = .039 for AP and .027 for RL dimensions) (Fig 2).

Not only were we not able to detect smaller FILs on VIBE/LAVA sequences, we also found that FILs measured smaller on VIBE/LAVA sequences compared with conventional T1 FSE sequences (Fig 1). As stated previously, the mean AP and RL diameters of FILs in T1 FSE images were 5.40 and 5.02 mm, respectively; however, the mean AP and RL diameters of the FILs as measured on the corresponding VIBE/LAVA images were 4.85 and 4.57 mm. These measurement differences were statistically significant (paired *t* test, *P* value = .003 for AP and <.001 for RL diameters), noting that the VIBE/LAVA sequence underestimates the actual size of the FILs (Fig 1).

By setting a cutoff point of 1.45 mm for FIL AP diameter, the VIBE/LAVA sequence detected FILs with a sensitivity of 75%

Table 2: Number, size, and extent of FIL each sequence detected

Sequence	FIL +ve	FIL +ve Mean AP	FIL +ve Mean RL	FIL +ve Mean CC
+T1 FSE and +VIBE/LAVA, measured in T1 FSE	21/22 (95.4)	5.4	5	3.8
+T1 FSE and +VIBE/LAVA, measured in VIBE/LAVA	12/22 (54.5)	4.9	4.6	2.2
+T1 FSE and −VIBE/LAVA, measured in T1 FSE	9/21 (42.9)	1.5	1.6	2.5

Note:—RL indicates right-left dimension; CC, craniocaudal dimension; FIL +ve, positive detection of a FIL; FIL −ve, negative detection of a FIL.

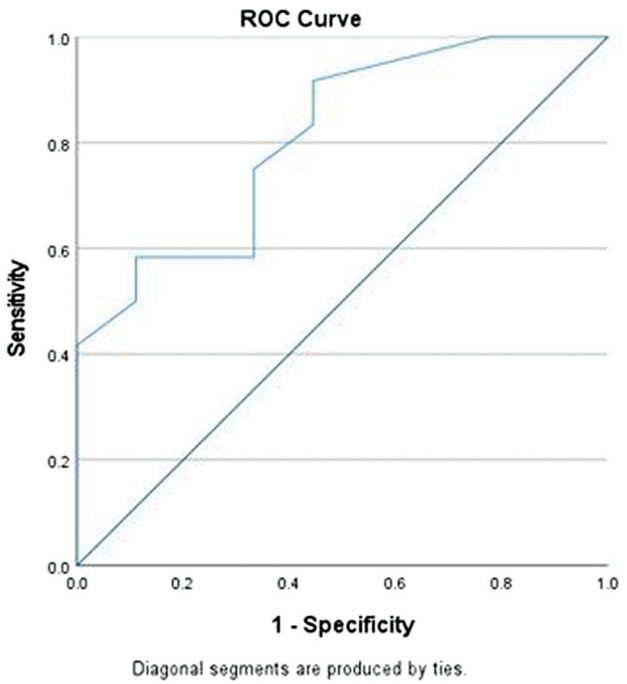

FIG 3. ROC curve for FIL AP diameter (area under the curve = 0.810, *P* value = .017).

and a specificity of 66.7% (ROC area under the curve = 0.810, *P* value = .017) (Fig 3). Considering the same sensitivity and specificity for the RL diameter, the cutoff point of 1.90 mm was optimal for this measurement (ROC area under the curve = 0.815, *P* value = .016) (Fig 4).

In addition to the size, we also compared the craniocaudal lengths of the FILs between the 2 sequences. The mean lengths of the FILs on the T1 FSE and VIBE/LAVA sequences were 3.75 and 2.17 vertebral levels, respectively. T1 FSE revealed larger craniocaudal extensions of FILs compared with the VIBE/LAVA sequence (paired *t* test, *P* value < .001).

The mean craniocaudal extent of FILs on the T1 FSE images of patients with positive findings on VIBE/LAVA was 1.3 levels longer than in those with negative findings. However, this difference was not statistically significant (independent *t* test, *P* value = .057).

The interrater reliability was measured by calculating the intraclass correlation coefficient. The intraclass correlation coefficient for the AP and RL diameter measurements for the T1 FSE sequences were 0.93 and 0.99, respectively, which are consistent with an excellent reliability. Similarly, we calculated the intraclass correlation coefficients for the same measurements for the VIBE/LAVA sequences, which were 0.89 for AP and 0.98 for RL, consistent with good and excellent reliability, respectively.

The intraclass correlation coefficients in measuring the FIL craniocaudal extension were 0.86 and 0.83 for T1 FSE and VIBE/LAVA sequences, respectively, indicating a good interrater reliability of these measurements.

DISCUSSION

The detection of FILs, either related to a fatty filum or an intrathecal lipoma, is clinically important for the assessment of suspected tethered cord. These congenital abnormalities impair spinal cord ascent and cause excessive stress on the conus.[6,7] Early detection and surgical intervention can help to alleviate symptoms and promote normal development in children.[20]

T1 FSE sequences have long been considered the criterion standard for the detection of fatty elements in the spine.[14] More recently, there has been an emphasis on the development of accelerated/fast sequences, leading to the development of fast, more motion-resistant sequences with decreased CSF pulsation artifacts, including 3D T1-weighted gradient-echo sequences such as VIBE/LAVA.[21] However, to date, few studies have investigated their role in the detection of FILs in pediatric spine imaging.

In 2013, Murakami et al[22] were the first to use the 3D T1-weighted spoiled gradient-echo sequence to detect lumbosacral lipoma and thickened filum terminales. The authors concluded that 3D T1 gradient-echo was superior to the conventional T1-weighted sequence in detecting thickened filar anomalies. The 3D T1 gradient-echo was able to localize the intrathecal lipoma in more section slices and clearly demarcated the filum terminal contour, allowing more accurate filum terminale diameter measurements.[22]

Our study sought to compare the utility of the VIBE/LAVA sequence with that of the conventional T1 FSE sequence for the detection of FILs. We found that FILs on VIBE/LAVA sequences were only detectable 54.5% of the time compared with 95.4% of the time on the conventional T1 FSE sequences. We found that FILs measuring approximately 1.5 mm in the axial plane could be detected on conventional T1 FSE sequences but not on the VIBE/LAVA sequences.

Moreover, FIL measurements made on VIBE/LAVA sequences were consistently smaller compared with those of the conventional T1 FSE sequences. In our study cohort, we had 1 patient who did not demonstrate evidence of a FIL on both the conventional T1 FSE sequence and the VIBE/LAVA sequence but had fatty elements identified at histopathology following a tethered cord release operation. This finding is supported in the literature noting microfatty elements in the filum terminale that were radiographically occult.[23,24]

There are several limitations to this study. The first being its retrospective nature. A retrospective design was utilized as we used the histopathology findings from tethered cord release surgery to validate the presence of fatty intrathecal tissue to validate the

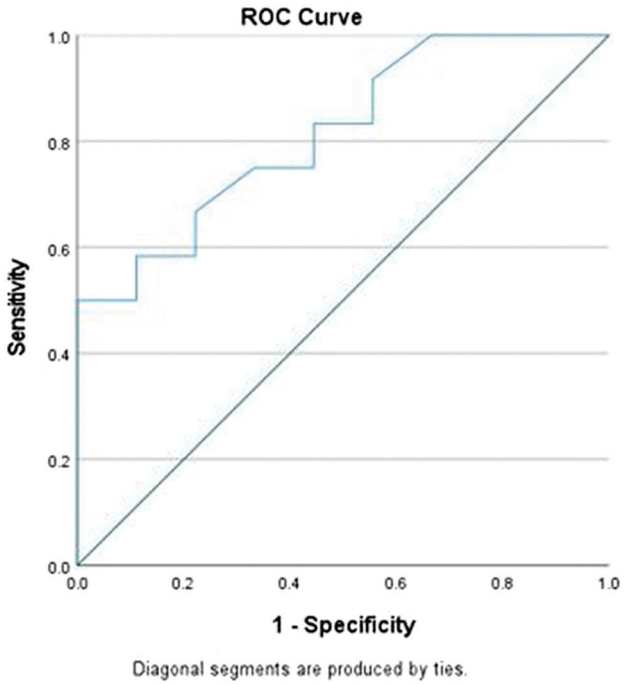

FIG 4. ROC curve for FIL RL diameter (area under the curve = 0.815, *P* value = .016).

findings on the conventional T1 FSE sequences and VIBE/LAVA sequences. Additionally, this study cohort was relatively small; however, we did have enough statistical power to perform our analyses (the calculated minimum number of subjects that needed to be enrolled to have 80% statistical power with $\alpha = .05$ was 16). The focus of this study is narrow in scope, being directed at the detection of fatty intrathecal components. We recognize that there are numerous other intrathecal and filar abnormalities that may result in a tethered cord. We thought that the narrow focus of this study emphasizes the importance of performing T1 FSE sequences over VIBE/LAVA sequences for the detection of small FILs.

CONCLUSIONS

The results of our study demonstrate improved sensitivity for detecting FILs on conventional T1 FSE sequences over the VIBE/LAVA sequences. While the VIBE/LAVA sequences are attractive to use, given motion resistance and decreased acquisition time, small FILs may be missed, potentially leading to delayed diagnosis and treatment.

Disclosure forms provided by the authors are available with the full text and PDF of this article at www.ajnr.org.

REFERENCES

1. Lew SM, Kothbauer KF. **Tethered cord syndrome: an updated review.** *Pediatr Neurosurg* 2007;43:236–48 CrossRef Medline
2. Solmaz I, Izci Y, Albayrak B, et al. **Tethered cord syndrome in childhood: special emphasis on the surgical technique and review of the literature with our experience.** *Turk Neurosurg* 2011;21:516–21 Medline
3. Sanchez T, John RM. **Early identification of tethered cord syndrome: a clinical challenge.** *J Pediatr Health Care* 2014;28:e23–33 CrossRef Medline
4. Gharedaghi M, Samini F, Mashhadinejad H, et al. **Orthopedic lesions in tethered cord syndrome: the importance of early diagnosis and treatment on patient outcome.** *Arch Bone Jt Surg* 2014;2:93–97 Medline
5. Chern JJ, Dauser RC, Whitehead WE, et al. **The effect of tethered cord release on coronal spinal balance in tight filum terminale.** *Spine (Phila Pa 1976)* 2011;36:E944–49 CrossRef Medline
6. Gupta A, Rajshekhar V. **Fatty filum terminale (FFT) as a secondary tethering element in children with closed spinal dysraphism.** *Childs Nerv Syst* 2018;34:925–32 CrossRef Medline
7. Al-Omari MH, Eloqayli HM, Qudseih HM, et al. **Isolated lipoma of filum terminale in adults: MRI findings and clinical correlation.** *J Med Imaging Radiat Oncol* 2011;55:286–90 CrossRef Medline
8. Rohrschneider WK, Forsting M, Darge K, et al. **Diagnostic value of spinal US: comparative study with MR imaging in pediatric patients.** *Radiology* 1996;200:383–88 CrossRef Medline
9. Tortori-Donati P, Rossi A, Biancheri R, et al. **Magnetic resonance imaging of spinal dysraphism.** *Top Magn Reson Imaging* 2001;12:375–409 CrossRef Medline
10. Mehta DV. **Magnetic resonance imaging in paediatric spinal dysraphism with comparative usefulness of various magnetic resonance sequences.** *J Clin Diagn Res* 2017;11:TC17–22 CrossRef Medline
11. Gewirtz JI, Skidmore A, Smyth MD, et al. **Use of fast-sequence spine MRI in pediatric patients.** *J Neurosurg Pediatr* 2020;26:676–81 CrossRef Medline
12. Sankhe S, Dang G, Mathur S, et al. **Utility of CISS imaging in the management of tethered cord syndrome.** *Childs Nerv Syst* 2021;37:217–23 CrossRef Medline
13. Khalatbari H, Perez FA, Lee A, et al. **Rapid magnetic resonance imaging of the spine in neonates with spinal dysraphism.** *World Neurosurg* 2020;144:e648–59 CrossRef Medline
14. Zugazaga Cortazar A, Martin Martinez C, Duran Feliubadalo C, et al. **Magnetic resonance imaging in the prenatal diagnosis of neural tube defects.** *Insights Imaging* 2013;4:225–37 CrossRef Medline
15. Park JE, Choi YH, Cheon JE, et al. **Three-dimensional radial VIBE sequence for contrast-enhanced brain imaging: an alternative for reducing motion artifacts in restless children.** *AJR Am J Roentgenol* 2018;210:876–82 CrossRef Medline
16. Wetzel SG, Johnson G, Tan AG, et al. **Three-dimensional, T1-weighted gradient-echo imaging of the brain with a volumetric interpolated examination.** *AJNR Am J Neuroradiol* 2002;23:995–1002 Medline
17. Koh E, Walton ER, Watson P. **VIBE MRI: an alternative to CT in the imaging of sports-related osseous pathology?** *Br J Radiol* 2018;91:20170815 CrossRef Medline
18. Bangiyev L, Raz E, Block TK, et al. **Evaluation of the orbit using contrast-enhanced radial 3D fat-suppressed T1 weighted gradient echo (Radial-VIBE) sequence.** *Br J Radiol* 2015;88:20140863 CrossRef Medline
19. Cho HH, Choi YH, Cheon JE, et al. **Free-breathing radial 3D fat-suppressed T1-weighted gradient-echo sequence for contrast-enhanced pediatric spinal imaging: comparison with T1-weighted turbo spin-echo sequence.** *AJR Am J Roentgenol* 2016;207:177–82 CrossRef Medline
20. Cools MJ, Al-Holou WN, Stetler WR Jr, et al. **Filum terminale lipomas: imaging prevalence, natural history, and conus position.** *J Neurosurg Pediatr* 2014;13:559–67 CrossRef Medline
21. Kralik SF, O'Neill DP, Kamer AP, et al. **Radiological diagnosis of drop metastases from paediatric brain tumours using combination of 2D and 3D MRI sequences.** *Clin Radiol* 2017;72:902e913–19 CrossRef Medline
22. Murakami N, Morioka T, Hashiguchi K, et al. **Usefulness of three-dimensional T1-weighted spoiled gradient-recalled echo and three-dimensional heavily T2-weighted images in preoperative evaluation of spinal dysraphism.** *Childs Nerv Syst* 2013;29:1905–14 CrossRef Medline
23. Tu A, Steinbok P. **Occult tethered cord syndrome: a review.** *Childs Nerv Syst* 2013;29:1635–40 CrossRef Medline
24. Rezaee H, Tavallaii A, Keykhosravi E, et al. **Effect of untethering on occult tethered cord syndrome: a systematic review.** *Br J Neurosurg* 2022;36:574–82 CrossRef Medline